



Classification of imbalance levels in a scaled wind turbine through detrended fluctuation analysis of vibration signals



Elineudo Pinho de Moura ^{a,*}, Francisco Erivan de Abreu Melo Junior ^b,
 Filipe Francisco Rocha Damasceno ^c, Luis Câmara Campos Figueiredo ^b,
 Carla Freitas de Andrade ^b, Maurício Soares de Almeida ^b, Paulo Alexandre Costa Rocha ^b

^a Departamento de Engenharia Metalúrgica e de Materiais, Universidade Federal do Ceará, 60440-554 Fortaleza, CE, Brazil

^b Departamento de Engenharia Mecânica, Universidade Federal do Ceará, 60455-760 Fortaleza, CE, Brazil

^c Departamento de Computação, Universidade Federal do Ceará, 60440-900 Fortaleza, CE, Brazil

ARTICLE INFO

Article history:

Received 23 October 2015

Received in revised form

4 April 2016

Accepted 4 May 2016

Available online 26 May 2016

Keywords:

Wind turbine

Imbalance

Vibration analysis

Detrended fluctuation analysis

Pattern recognition

ABSTRACT

This work proposes to identify different imbalance levels in a scaled wind turbine through vibration signals analysis. The experiment was designed in such a way that the acquired signals could be classified in different ways. A combination of detrended fluctuation analysis of acquired signals and different classifiers, supervised and unsupervised, was performed. The optimum number of groups suggested by k-means clustering, an automatic classifier with unsupervised learning algorithm, differs from the number of classes (or subsets) defined during the experimental planning, presenting another approach to the possible classification of vibration signals. Additionally, three supervised learning algorithms (namely neural networks, Gaussian classifier and Karhunen-Loève transform) were employed to this end, classifying the collected data in some predefined amounts of classes. The results obtained for the test data, just a little different regarding the training data, also confirmed their capability to identify new signals. The results presented are promising, giving important contributions to the development of an automatic system for imbalance diagnosis in wind turbines.

© 2016 Elsevier Ltd. All rights reserved.

1. Introduction

A better understanding about the fields of global warming and climate change is the way for renewable energy sources to become a main concern for governments and international organizations and institutions. Therefore, the search for new alternative sources of energy has become the key to ensure a sustainable future. In this scenario, it is well established that renewable energy sources provide substantial benefits. Among various renewable energy sources such as solar, biomass, geothermal and hydraulic, wind stands out as a clean, efficient and promising alternative with little environmental impact.

Improvements on wind turbines reliability and performance are essential. Although potential problems can occur in any component of a wind turbine, the most common failures are presented on its rotor blades or tower. So, special attention must be paid to the

mechanical effects of wind action on rotor blades to avoid excessive stresses, instability, fatigue and rupture. The harmful consequences from mechanical vibrations have been extensively studied by various researchers worldwide, e.g. Refs. [2,13]. Over the years, vibration analysis has been performed by using signal processing, e.g. Refs. [7,14,15,23,27,33,34,36,46].

One of the major concerns regarding a wind turbine is the negative effect of vibrations on its performance. Therefore, many researchers have paid much attention to mitigating and controlling vibrations on wind turbines [47]. investigated the performance of roller dampers for mitigation of edgewise vibrations on rotating wind turbine blades and his results indicated that the proposed damper could effectively improve the structural response of wind turbine blades [16]. showed a new active control strategy designed and implemented to control the in-plane vibration of large wind turbine blades which, in general, is not aerodynamically damped. It was concluded that the use of the proposed new active control scheme significantly reduces the in-plane vibration of large, flexible blades.

A nonlinear dynamic model was developed by Ref. [48] to study

* Corresponding author.

E-mail address: elineudo@ufc.br (E.P. de Moura).

the torsional vibrations of wind turbine gearboxes having two planetary gear stages and one parallel gear stage. Many factors acting on the dynamic behavior of wind turbine gearbox components are considered by employing the numerical integration method. It was found that the external excitation is the most important influence on the torsional vibrations of wind turbine gearbox components.

In their work [40], proposed a model to control wind turbine vibrations by changing the rotational speed of the blades and a multi-modal mathematical model describing the dynamics of flexible rotor blades and their interaction with the turbine tower, all being formulated by using a Lagrangian approach. An active controller based on active tendons was proposed to mitigate wind-induced edgewise vibrations.

Feature extraction and fault diagnosis via vibration analysis is a common and effective mean for wind turbine condition monitoring, specially on rotation parts, as well as blade-cabin-tower coupling system [24]. calculated tower natural frequency based on the coordinate system. Wind-induced random vibration was analyzed and total wind force on blade-cabin-tower coupling system was determined.

[1] used a novel approach called Empirically Decomposed Feature Intensity Level (EDFIL) to identify the fault severity caused by intentionally produced cracks of different sizes in a wind turbine blade. He also showed that common vibration analysis techniques, such as Kurtosis, Root Mean Square, Crest Factor and Fast Fourier Transform (FFT) are not useful tools to diagnose wind turbine blade defects. As it was explained, more advanced monitoring techniques are required to deal with noise-contaminated and non-stationary signals of a wind turbine.

A combination of Detrended Fluctuation Analysis (DFA) and pattern recognition techniques was successfully applied to fault diagnosis in gearbox [12] and bearing [11] under various conditions of frequency, load and severity or kind of fault. Inspired by these previous works and taking into account the relevance of the above discussed subjects, this study performs a similar approach. The idea is to investigate whether this approach can be useful in the classification of vibration signals acquired from a scaled wind turbine and to evaluate the performance of different pattern recognition techniques.

2. Experimental setup

In this work, a set of blades with NREL S809 profile, specifically developed for use in horizontal-axis wind turbines (HAWTs), was designed by a in-house developed software [9], which uses a methodology of design from Ref. [3] to calculate the blades parameters, such as the chord and twist distribution, as shown by the images on Fig. 1. The blades were manufactured using a stereolithography technique, commonly called 3D printing, which guarantees the production of balanced blades, and after a polishing process the roughness can be negligible. Three blades were built, each with 0.20 m length, 15 g and tip speed ratio λ equal to seven.

The experiments were carried out on a bench composed of a wind turbine shaft and a three-bladed rotor, a torque transducer and an electric motor, as shown in Fig. 2. This bench was located in an open circuit subsonic wind tunnel approximately 6.5 m long with a test section of 0.50×0.50 m, powered by a 1.49 kW (2 hp) exhauster. To guarantee that the blades work in their tip speed ratio (λ) of project, the rotor remained at a constant rotation of 900 rpm and the mean wind velocity at the test section was 2.71 m/s with standard deviation of 0.035 and turbulence level below 2%. The blockage ratio found in the test section was 50.77% and the blockage factor required for correction of C_p (power coefficient)

calculation was 0.84 [5].

The aim of the present work is to verify if the approach successfully applied in previous fault diagnosis works can be useful to distinguish unbalanced levels of scaled wind turbine. Given that, the following main work conditions were regarded:

1. Imbalance on a single blade by mass addition. This condition reproduces several situations, such as accumulated dirt over a blade or any object attached to it. This condition was simulated by mass addition (0.5, 1.0 and 1.5 g) at the tip of only one blade.
2. Imbalance on a single blade by lacking mass. This condition reproduces the possibility of a broken blade or excessive weight loss on a blade. This condition was simulated by mass addition (0.5, 1.0 and 1.5 g) at the tip of two blades.
3. Balanced system. This normal condition can be obtained in two different ways: when all blades are of same mass and their rotor is balanced, or by using only the shaft. These configurations also help us to certify the balance of the system.

In addition, a question can be formulated concerning the most adequate amount of classes to be used for this setup. Three groups as the main work conditions, as well as seven (and even eight) groups as subsets are possible answers. For all test conditions, rotor remained at a constant rotation of 900 rpm.

Signals were captured through a Bruel & Kjaer accelerometer, model 4381V, which is located in the shaft bearing closer to the blades, as shown in Fig. 2. The sensor is coupled to a Bruel & Kjaer amplifier, model 2692. For band filtering, 1.0 Hz (high) and 100.0 Hz (low) were chosen as limits. Afterwards, a Tektronix oscilloscope, model 1062 TBS, was used to record signals. Each signal was composed of 500 data points acquired with a sampling rate of 250 Hz (250 samples/s). For all tested conditions, rotor remained at a constant rotation of 900 rpm. For each balanced level, 50 vibration signals were captured, resulting in a dataset of 400 vibration signals. Fig. 3 shows a representative normalized vibration signal.

The Nyquist sampling theorem affirms that, to be possible to recover all spectral components of a periodic waveform, the sampling rate must be at least twice the highest waveform frequency. So that, the higher the sampling rate the higher the recorded frequencies. With this in mind, and considering that the rotation frequency of wind turbine is 900 rpm (15 rps), the minimum sampling rate to record these signals should be 30 Hz. However, vibration signals are not a single periodic waveform and they have upper spectral components. In addition, the sampling rates offered by oscilloscope is limited. Some of the sampling rates offered are 25, 50, 125, 250 Hz and go on. The first one do not satisfy the Nyquist sampling theorem. In order to avoid missing of those important spectral components to vibration signal analysis, they were recorded at 250 Hz. On the other hand, the recording of frequency beyond the frequencies observed in Fourier spectrum of the signal is unnecessary.

3. Detrended fluctuation analysis

Detrended Fluctuation Analysis, or DFA [31], aims to improve the evaluation of correlations in a time series by eliminating trends in the data. The method assumes a profile that consists of an integrated series y_j

$$y_j = \sum_{i=1}^j (u_i - \langle u \rangle) \quad (1)$$

where $\langle u \rangle$ is the overall average of the original series,

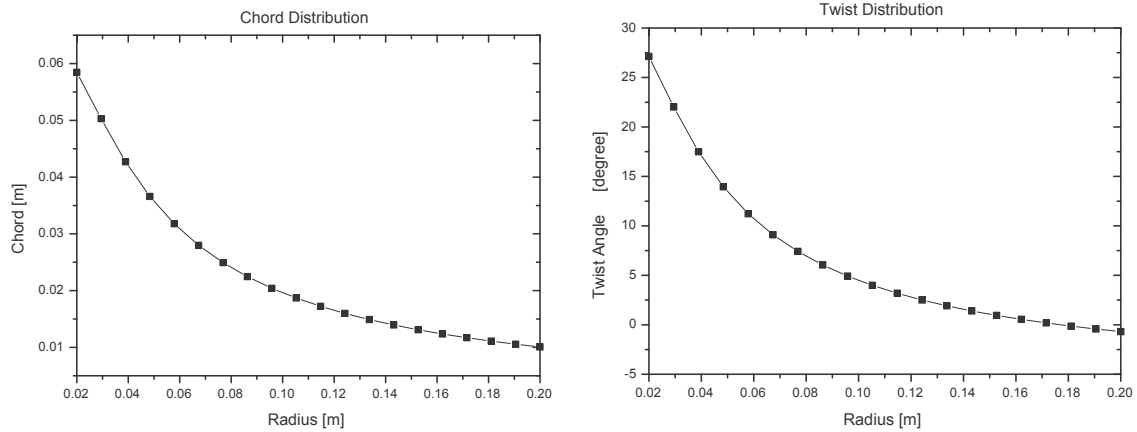


Fig. 1. Chord and twist distributions.

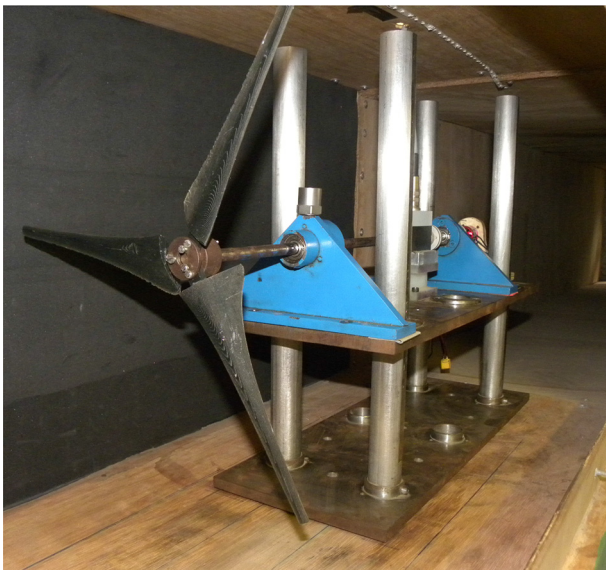


Fig. 2. Scaled wind turbine and measurement apparatus for a wind tunnel test.

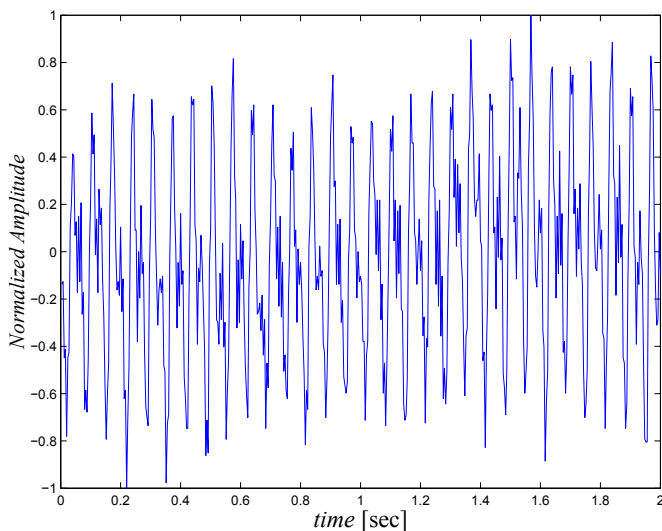


Fig. 3. Normalized vibration signal obtained from a scaled wind turbine with a single unbalanced blade at a rotation frequency of 900 rpm on a wind tunnel.

$$\langle u \rangle = \frac{1}{N} \sum_{i=1}^N u_i \quad (2)$$

For each profile, DFA involves performing a polynomial data fitting within intervals of size τ and evaluating the corresponding detrended fluctuations defined as the difference between the integrated series y_j and the local trend \tilde{y}_j . In this work it was applied a first-order DFA scheme which means a first-degree polynomial. A curve of the average fluctuation as a function of size interval τ is built by repeating this procedure for many interval sizes. Non-overlapping intervals are a common practice. However, since the series length N is not a multiple of the interval size, losing a small part at the end of the profile is likely to occur. To get over this problem, the solution firstly proposed by Ref. [35] using overlapping time windows was applied. Thus, for each interval I_k the variance of the residuals was calculated as

$$f_k^2(\tau) = \frac{1}{\tau - 1} \sum_{i \in I_k} (y_i - \tilde{y}_i)^2 \quad (3)$$

Finally, the covariance $F(\tau)$ was calculated by summing over all overlapping $N - \tau + 1$ windows of size τ .

$$F(\tau) = \frac{1}{N - \tau + 1} \sum_k f_k(\tau) \quad (4)$$

From the values of $\log_{10}(F(\tau))$, vectors whose components correspond to the average fluctuation associated with suitably chosen interval sizes can be defined. In this work, window sizes ranging the integer part of the integer powers of $2^{\frac{1}{4}}$, i.e. from 5 to 250, were used. In this sense, each vector had 24 components and the values of τ corresponded to the values in (5,6,7,8,9,11,13,16,19,22,26,31,37,44,53,63,74,88,105,125,149,177,210, 250). (see Fig. 4).

Given the length of signals and the sampling rate used during their recordings, each signal corresponds to a time series with just 2 s. Although wind turbines do not operate at steady state conditions or uniform wind regimes, at short time scales it is possible to consider a quasi-steady state.

Furthermore, a number of results indicates that DFA, a tool originally developed to differentiate between local patchiness and long-range correlations in DNA sequences [32], can be quite useful in the study of non steady state time series such as characterization

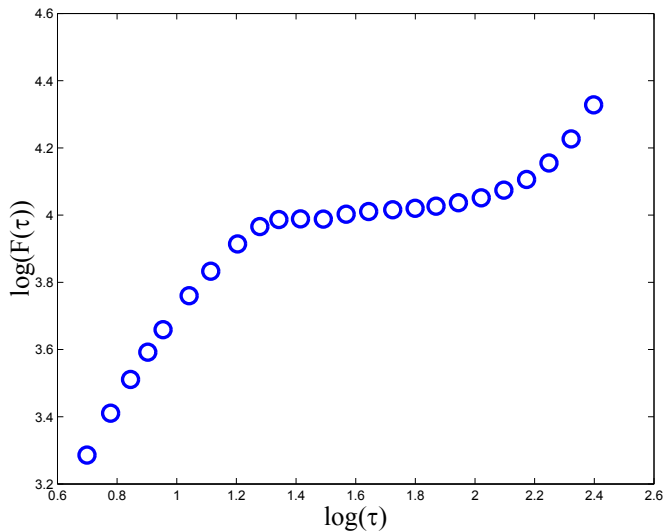


Fig. 4. Representative DFA curve obtained from signal displayed on Fig. 3.

of cast iron microstructure based on ultrasonic backscattered signals [10,26], classification of welding defects based on TOFD ultrasonic signals [42], gear fault diagnosis based on vibration signals [12], monitoring of metal transfer modes in mig/mag welding based on voltage and current time series [43] and characterization of microstructural changes in coarse ferritic-pearlitic stainless steel based on magnetic Barkhausen noise and magnetic flux signals [29].

This type of analysis has also been widely used in the study of random non-stationary series, ranging from seismic [41] and climate data [22] to financial data [4] and in the study of different music genres [21], as well as long-term correlations in wind speed (citegovindan2004). Another previous work goes as far as of investigating the impact of the wake effect upon the steady-state of a wind farm [17].

4. K-means clustering

As a new approach, not found in the literature for this type of problem, the vectors resultant from DFA were grouped using clustering techniques. In this study, we called vector each curve with values of $\log_{10}(F(\tau))$ obtained after a DFA of vibration signals, as the one portrayed in Fig. 3. Each curve is represented by a vector of dimension 24 (one curve with 24 points), or geometrically, by one point in a space of dimension 24. These vectors constitute the input of k-means.

Clustering is an unsupervised approach in which, given a dataset, it aims to create groups, which are subsets of the initial dataset. It is expected that elements of a same group are similar and elements of different groups are as different as possible. In multidimensional datasets, the concept of similarity between two points can be built based on the dissimilarity, which can be set as the distance between them. Thus, the closer the points, the more similar they are.

For the clustering approach, the k-means method was applied. K-means is a partitional clustering algorithm widely known in machine learning. Partitional clustering aims to directly decompose the dataset into disjoint clusters by optimizing a cost function (or criterion function), which emphasizes the desired structure of the data. For example, using different distance norms (Euclidean, Manhattan, Chebyshev) may result in different cost functions, thus yielding different resulting clusters [39].

K-means can be applied when the amount of clusters to be

generated is already defined. In this sense, some clustering evaluation techniques can be applied to decide how many clusters should be used. Two indexes were evaluated to help this decision: Silhouette and Davies-Bouldin. Both indexes try to measure how well different clusters are separated from each other and how well elements of a same cluster are grouped.

K-means idea was first introduced by Lloyd in 1957, though it would only be published years later [25]. This iterative method represents each cluster by a single point called centroid, and decides to which cluster each data point belongs by checking the distance from the data point to each centroid, selecting the smaller distance. The use of centroids to compare distances instead of comparisons between each pairs of points in the dataset reduces its complexity, while having good resulting clusters [37].

Consider $\mathbf{X}_{n \times p}$ a p -dimensional dataset with n samples and suppose we grouped these data in k groups $\mathbf{S}_1, \mathbf{S}_2, \dots, \mathbf{S}_k$. Based on the idea of choosing the smaller distance from a point to a centroid, k-means' cost function evaluates the clustering by checking the distances from each element to the centroid of the cluster to which it belongs via the following cost function:

$$Q = \sum_{i=1}^k \sum_{j=1}^n u_{ij} D_p^2(\mathbf{c}_i, \mathbf{x}_j) \quad (5)$$

where $u_{ij} = 1$ if $\mathbf{x}_j \in \mathbf{S}_i$ and $u_{ij} = 0$ otherwise, and $D_p^2(\mathbf{c}_i, \mathbf{x}_j)$ is the squared p -dimensional Euclidean distance between \mathbf{c}_i and \mathbf{x}_j . K-means, then, is an iterative method for associating every data point \mathbf{x}_j , $j = 1, \dots, n$, to the cluster with the nearest centroid, and updating every centroid \mathbf{c}_i , $i = 1, \dots, k$, as the mean of the cluster \mathbf{S}_i . The convergence can be checked by analyzing the changes between configurations, in such a way that if there's no significant change between two consecutive iterations of the algorithm then convergence is achieved.

Despite of its good results and small complexity, the basic k-means algorithm may outcome some problems. First, while setting the initial centroids, a somewhat distant centroid (from the dataset) can be set. This may result in an empty cluster, and then the algorithm would be grouping in $k-1$ groups instead of k . To solve this problem, k different points from the dataset will be chosen, implying that each group will contain at least one element of the dataset.

Another problem is the previous requirement of the groups quantity k . This may be troublesome when one is not sure about how many groups should exist. There are some techniques which can be applied to the dataset that are able to indicate the number of clusters. In this paper, the Silhouette and Davies-Bouldin (DB) indexes are applied.

The idea used within both Silhouette and Davies-Bouldin indexes is that a cluster is considered "bad" if it's very close to another cluster (meaning that the clusters could be put together) or if its elements are too spread (meaning that some distant elements could belong to another cluster). That is, if a cluster is distant from other clusters and if it has dense groups of elements, it can be classified as a "good" cluster.

Both indexes are applied over a configuration (resulting from an execution of a clustering algorithm) to analyze how good this configuration is. Their output can be used to choose the optimal number of clusters to use on a clustering algorithm.

Silhouette index was introduced by Ref. [38]. This index is applied over a configuration to evaluate how well every element is individually grouped, and it uses the index of every element to evaluate the configuration. Using the above procedure, for every data point Silhouette index checks how near the point is from the elements of its group, and how near the point is from elements of

its neighbour group (the nearest cluster from the point that isn't its own cluster).

Consider a single point \mathbf{x} . Let $a(\mathbf{x})$ be the mean of the distances from \mathbf{x} to each other element from the same cluster as \mathbf{x} . Let $b(\mathbf{x})$ be the mean of the distances from \mathbf{x} to every element from \mathbf{x} 's neighbour cluster. Let $s(\mathbf{x})$ be the Silhouette index of \mathbf{x} , defined as:

$$s(\mathbf{x}) = \frac{b(\mathbf{x}) - a(\mathbf{x})}{\max(b(\mathbf{x}), a(\mathbf{x}))} \quad (6)$$

Clearly we can see that $-1 \leq s(\mathbf{x}) \leq 1$. Silhouette considers higher values of $b(\mathbf{x})$ as a signal of good configuration, while considers higher values of $a(\mathbf{x})$ as a signal of bad configuration. One can read this by checking that a point close to other elements of its cluster is a well grouped element, and a point distant from its neighbour cluster is well separated from other clusters. Thus, higher values of $s(\mathbf{x})$ mean that the element is well grouped, while lower values of $s(\mathbf{x})$ mean the element isn't well grouped, regardless of the way this clustering was established.

Based on a dataset $\mathbf{X}_{n \times p}$ and the configuration (resulting from a clustering algorithm), every $s(\mathbf{x}_j)$, $j = 1, \dots, n$, is computed to evaluate the configuration by evaluating the Silhouette index SI as the mean of the Silhouette indexes $s(\mathbf{x}_j)$. Therefore $-1 \leq SI \leq 1$, where higher values are signal of good configurations and smaller values indicate bad configurations.

The Davies-Bouldin index (or DB index) was introduced by Ref. [8]. This index is also applied over a configuration, but it calculates the index of every cluster to evaluate the configuration. For every cluster, it can be analyzed through the DB index by the mean of the distance from a cluster's centroid to its elements and by the distance between each pair of centroids. DB index also uses centroids to calculate the distances, which reduces its computational complexity when compared to Silhouette.

Consider a hypothetical configuration. Let \mathbf{c}_i be the centroid of the cluster \mathbf{S}_i . Let d_i be the mean of the distances between \mathbf{c}_i and every other point belonging to \mathbf{S}_i . Let $d(\mathbf{c}_i, \mathbf{c}_j)$ be the distance between \mathbf{c}_i and \mathbf{c}_j . Let DBI be the Davies-Bouldin index of the configuration, defined as:

$$DBI = \frac{1}{k} \sum_{i=1, i \neq j}^k \max \left(\frac{d_i + d_j}{d(\mathbf{c}_i, \mathbf{c}_j)} \right) \quad (7)$$

Through Davies-Bouldin, the configuration can be evaluated by using the distances both within and between clusters. Using the same idea of Silhouette, a smaller within-cluster sum of distances means its elements are well united, which is an indicative of a good cluster. Higher distances between centroids of different clusters are also an indicative of a good cluster, since it shows that clusters are well separated from each other.

Therefore, for every cluster \mathbf{S} , DB index looks for another cluster \mathbf{S}' that maximizes the spreading of both clusters while minimizing the distance, thus selecting the cluster that could be produced by errors in the clustering process. Hence, smaller values of DBI indicate better configurations.

The acquired dataset can be brought together in different ways, so both Silhouette and DB indexes were used to decide in how many clusters the dataset should be grouped. For this task, k-means was used as the clustering algorithm. With the algorithm's output vector \mathbf{k} , we choose the optimal value of k as the amount of clusters that was most recommended as optimal. The concept within the algorithm is to get a good clustering result from k-means, and calculate the Silhouette and Davies-Bouldin indexes over it. K-means was run 100 times to guarantee that a good clustering might be achieved. Then, this process was repeated for each number of clusters in $(2, \dots, 20)$, resulting in heaps of indexes.

The optimal value for each index (the maximum value for Silhouette and the minimum value for Davies-Bouldin) was selected and the minimum suggested number of groups was picked between the two optimal as the recommended number of clusters. The choice of the optimal value of k was made based on the approach presented on Algorithm 1. Choosing either minimum or maximum values between the optimals gives approximately the same result. To ensure the precision of the result, this test was repeated 1000 times, selecting 1000 optimal numbers of clusters. In all tests, the optimal (recommended) number of classes returned was 4.

Algorithm 1: Choice of the optimal number of clusters

Data: dataset $\mathbf{X}_{n \times p}$ (our dataset consists of $n = 400$ samples with $p = 24$ dimensions each)

Result: vector \mathbf{k} with occurrences of optimal number of clusters

```

1 set  $k_{max}$  as  $\lfloor \sqrt{n} \rfloor$ 
2 set  $\mathbf{k}$  as a  $k_{max}$ -dimensional vector of zeros, used to check how many times the amounts of clusters are suggested as the optimal
3 for  $it \leftarrow 1$  to 1000 do
4   set  $\mathbf{SI}$  and  $\mathbf{DB}$  as vectors to store the indexes for  $k = 2, \dots, k_{max}$  for iteration  $it$ 
5   for  $k_{it} \leftarrow 2$  to  $k_{max}$  do
6     run 100 full executions of k-means, grouping  $\mathbf{X}$  in  $k_{it}$  clusters and collecting 100 resulting configurations
7     from the 100 configurations, select the one that minimizes the value of k-means cost function
8     compute the Silhouette and Davies-Bouldin indexes for the selected configuration, resulting in two indexes for  $k_{it}$  clusters to be stored in  $\mathbf{SI}$  and  $\mathbf{DB}$ 
9   end
10  based on the maximum value in  $\mathbf{SI}$  and the minimum value in  $\mathbf{DB}$ , select  $k_{DB,opt}$  and  $k_{SI,opt}$  as the number of clusters considered optimal by each method
11  select the optimal number of clusters  $k_{opt}$  as  $\min(k_{DB,opt}, k_{SI,opt})$ 
12  increment  $\mathbf{k}[k_{opt}]$ , meaning  $k_{opt}$  was pointed once more as optimal
13 end
```

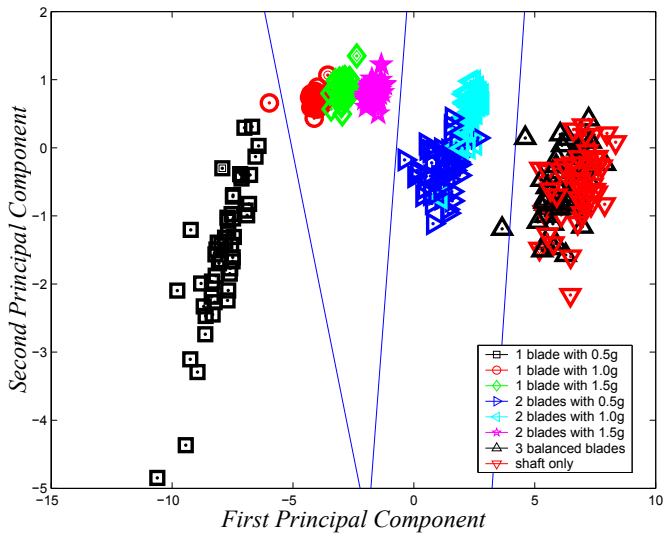


Fig. 5. Groups configuration resulting from k-means clustering with $k=4$ groups, overlapped to a Principal Component Analysis of DFA vectors of vibration signals. Groups are partitioned according to a Voronoi diagram.

In Fig. 5, PCA (Principal Component Analysis) was applied to reduce the original 24-dimension dataset in a 2-dimension one, making it easier to understand a plot of the dataset. PCA was introduced by Ref. [30] and the method aims to remove correlations on a dataset and, optionally, to reduce the dimension of the system while keeping a percentage of its information. In the plot presented by Fig. 5, the reduction was carried out from 24 to 2 dimensions and kept 99.26% of the information from the original dataset.

Based on the optimal value of k , we then executed k-means to group the data in $k=4$ groups. Each of the 4 centroids were initialized as different points out of the dataset. As the resulting clustering is affected by the choice of the initial centroids, some of them can be different than others, so it was chosen the most repeated configuration over 100 executions of k-means (which is also the configuration with the minimum value for k-means' cost function). The groups are as presented in Fig. 5.

For the following analysis, for the sake of simplicity, consider the nomenclature presented in Table 1.

The optimal configuration shows 4 groups, where k-means kept C1 as G1 and grouped C2, C3 and C6 in G2, C4 and C5 in G3, and C7 and C8 in G4. G1 is a group with a single, slightly heavier blade when compared to the others. G2 is a group representing a scenario with either one or two much heavier blades. G3 is a group with two slightly heavier blades when compared to the last one. G4 is a group representing the balanced scenario, either with 3 balanced blades or with no blades (shaft only).

We can then analyze how k-means detected groups by checking the classes of each group. G4 is a group of balanced scenarios, resulting in the smallest vibration. G1 is a group with a lightly

unbalanced scenario, where one of the blades is slightly heavier than the others, resulting in some more vibration. G3 is a group with a lightly unbalanced scenario where two of the blades are slightly heavier than the other, resulting in some vibration but being more stable than G1, probably due to the difference of weight.

Meanwhile, G2 is the group of most unbalanced scenarios, where big weights are applied to the blades (one blade in C2 and C3, and two blades in C6), resulting in higher vibrations when compared to other groups. It is worth pointing that G2 includes C2 but doesn't include C5. One possible explanation to this fact resides on the weight difference of the system, which results in better stability.

With the purpose of verifying the optimum number of classes and to make an automatic classification, a cluster analysis technique was employed. This can be useful when the classes of input data are not known and consequently the training procedure is not possible. Besides, since the number of classes and to which class each signal belongs are well known, supervised classifiers can also be employed.

5. Supervised classification

Three pattern recognition techniques (namely neural network, Gaussian discriminant and Karhunen-Loève) were used to classify the vectors obtained from the DFA of vibration signals according to different work conditions. A brief discussion of each technique is presented below. A similar approach was successfully applied to fault diagnosis of both gearbox [12] and bearing [11], to characterization of cast iron [10], and modeled microstructure from ultrasound signals [28].

5.1. Neural network

The basic unit of a neural network is the neuron, which is a mathematical operator that performs a linear combination of the inputs. Before this weighted sum is sent to an activation function, a bias may be added to it. Then a neuron can be represented as:

$$y = \phi \left(\sum_{i=1}^n w_i x_i + b \right) \tag{8}$$

where ϕ is the activation function, x_i are the input data, w_i are the synapse weights and b is the bias. This approach can be used to classify linearly separated data. However, several processes have nonlinear nature. Neurons disposed in layers, with each layer fully connected to the next one, compose a multilayer perceptron [18,44]. Multilayer perceptrons are able to classify nonlinearly separated data, but any nonlinear input-output mapping can be obtained by using a single hidden layer [6,19,20].

The estimation process is accomplished in two main steps. First, the network is trained with a set of input and output pairs. During this crucial stage, the weights of neurons are adjusted. The most common training method used is the backpropagation algorithm, which attempts to minimize the output error. Training is followed by the testing step, where the network is exposed to new data.

In this work, a neural network was implemented by a multilayer perceptron composed by an input layer with 24 neurons (the dimension of our vectors), one hidden layer and one output layer. The number of neurons in both hidden and output layers was changed according to the predefined number of classes, such that each class is distinguished by one neuron on the output layer and the number of neurons in the hidden layer is calculated by the floor of the mean between the number of dimensions of the data and the amount of classes to be used.

Table 1
Nomenclature of classes of imbalance.

Class	Added mass	Blade weight percentual
C1	0.5 g to one blade	3.33%
C2	1.0 g to one blade	6.67%
C3	1.5 g to one blade	10%
C4	0.5 g to two blades	3.33%
C5	1.0 g to two blades	6.67%
C6	1.5 g to two blades	10%
C7	three blades balanced (no mass added)	0%
C8	shaft alone	0%

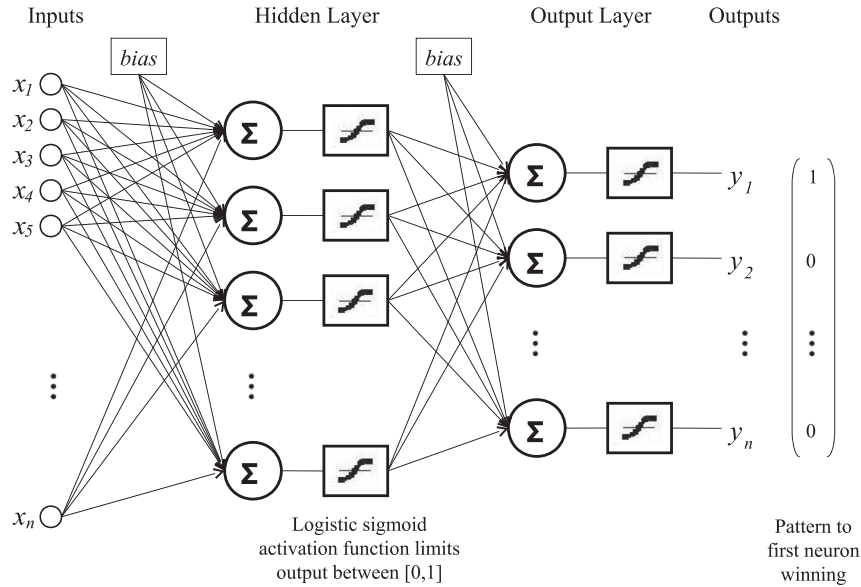


Fig. 6. Basic sketch of a neural network.

In an attempt to answer the starting question introduced in the experimental setup, the numbers of classes were chosen as 3 and 7, resulting in a hidden layer with 13 and 15 neurons, respectively. The connection weights between neurons in contiguous layers are adjusted so as to minimize the mean squared error between the desired and the actual outputs, according to the backpropagation prescription. Logistic sigmoid activation functions were used in all the neurons. In all cases, the input vectors (DFA results) were presented 1000 times, i.e., 1000 epochs of training were conducted. A basic sketch of a neural network is shown on Fig. 6.

5.2. Gaussian classifier

The Gaussian function is also a method that uses a supervised learning. This function works by classification of the d -dimensional vectors and training by supervised learning [45]. The general p -dimensional Gaussian density function for a given class i is given by:

$$p(\omega_i) = \frac{1}{(2\pi)^{\frac{p}{2}} |\mathbf{S}_i|^{\frac{1}{2}}} \exp \left[-\frac{1}{2} (\mathbf{x} - \mathbf{m}_i)^T \mathbf{S}_i^{-1} (\mathbf{x} - \mathbf{m}_i) \right] \quad (9)$$

Table 2

Average performance of the classifiers when applied over vectors built from recorded signals to classify the data in 3 classes, calculated over 100 sets of training and testing vectors. For each column, numbers indicate the percentage of vectors which were correctly classified; values in parenthesis correspond to the standard deviations; the values after '#' registers average misclassification rates (e.g. for class 1, #2:0.57 indicates that 0.57% of vectors belonging to class 1 were misclassified as belonging to class 2).

Class	Neural network		Gaussian		Karhunen-Loève	
	Training	Testing	Training	Testing	Training	Testing
1	100	99.43 (1.25) #2:0.57	100	98.87 (1.71) #2:1.13	100	100
2	100	100	95.65 (1.72) #1:4.35	94.93 (3.96) #1:5.07	99.90 (0.27) #1:0.1	99.53 (1.16) #1:0.47
3	100	100	100	100	100	100
Overall average	100	99.79	98.37	97.68	99.96	99.83

where \mathbf{x} denotes an input vector generated during the detrended fluctuation analysis, \mathbf{S}_i is the covariance matrix associated to class i and \mathbf{m}_i is the mean vector, also associated to class i , which in turn are given respectively by

$$\mathbf{S} = \frac{1}{n} \sum_{i=1}^n (\mathbf{x}_i - \mathbf{m})(\mathbf{x}_i - \mathbf{m})^T \quad (10)$$

and

$$\mathbf{m} = \frac{1}{n} \sum_{i=1}^n \mathbf{x}_i \quad (11)$$

where n is the amount of d -dimensional vectors \mathbf{x}_i associated to class i and T denotes the transpose vector. When $\mathbf{x} = \mathbf{m}_i$ the gaussian density function has its maximum value and the increase of the distance between \mathbf{x} and \mathbf{m}_i decreases the output of the function.

Using the training set, the mean and the covariance of the gaussian function are calculated for each class. Finally, using the testing set, the performance of the gaussian classifier in discriminating the vectors could be evaluated. The classifier discriminates each datum by associating each vector to the class with the highest output, obtained from the different gaussian density functions associated to each class.

As the vectors produced by the DFA of vibration signals are selected to define the sets of training and testing, a discussion about the success rate of Gaussian classifier in identification of each unbalancing level studied is made below in Section 5.4.

5.3. Karhunen-Loève transformation

For the Karhunen-Loève transformation (KLT), at first, the projection of training vectors along the eigenvectors of the intra-class covariance matrix \mathbf{S}_w , is defined as [45]:

$$\mathbf{S}_w = \frac{1}{n} \sum_{k=1}^{n_c} \sum_{i=1}^{n_k} y_{ik} (\mathbf{x}_i - \mathbf{m}_k)(\mathbf{x}_i - \mathbf{m}_k)^T \quad (12)$$

where n is the number of samples of the dataset, \mathbf{x}_i is the column

Table 3
Average performance of the classifiers for the generation of 7 classes. Classifiers' results are presented as in Table 2.

Class	Neural network		Gaussian		Karhunen-Loève	
	Training	Testing	Training	Testing	Training	Testing
1	100	100	100	100	100	100
2	100	100	100	97.80 (4.14) #1:0.3 #4:1.9	100	100
3	100	97.40 (4.39) #6:2.6	100	99.20 (3.06) #6:0.8	100	100
4	100	96.10 (6.15) #5:3.9	100	100	100	100
5	99.67 (0.84) #4:0.33	96.50 (5.36) #4:3.5	100	99.80 (1.40) #4:0.2	100	100
6	100	99.40 (2.37) #2:0.6	100	97.70 (4.66) #4:2.3	100	99 (3.0) #2:1
7	100	100	100	100	100	100
Overall average	99.96	98.67	100	99.31	100	99.88

vector corresponding to the i -th signal, n_c is the number of classes, n_k is the number of vectors of class k , \mathbf{m}_k is the mean vector of class k and T denotes the transpose vector. The element y_{ik} is equal to one if \mathbf{x}_i belongs to class k , and zero otherwise.

The resulting vectors undergo a re-scaling operation by a diagonal matrix built from the eigenvalues (λ_j) of \mathbf{S}_w . This operation can be written in matrix form as follows:

$$\mathbf{X}' = \Lambda^{-\frac{1}{2}} \mathbf{U}^T \mathbf{X} \quad (13)$$

where \mathbf{X} is the matrix whose columns are the training vectors \mathbf{x}_i , $\Lambda = \text{diag}(\lambda_1, \lambda_2, \dots)$ is the matrix of variances of the transformed features (eigenvalues of \mathbf{S}_w) and \mathbf{U} is the matrix whose columns are the eigenvectors of \mathbf{S}_w .

Finally, to compress the class information, the resulting vectors are projected onto the eigenvectors of the between-class covariance matrix \mathbf{S}_B , calculated as:

$$\mathbf{S}_B = \sum_{k=1}^{n_c} \frac{n_k}{n} (\mathbf{m}_k - \mathbf{m})(\mathbf{m}_k - \mathbf{m})^T \quad (14)$$

where \mathbf{m} is the overall mean vector. The full transformation can be written as:

$$\mathbf{X}'' = \mathbf{V}^T \Lambda^{-\frac{1}{2}} \mathbf{U}^T \mathbf{X} \quad (15)$$

where \mathbf{V} is the matrix whose columns are the eigenvectors of \mathbf{S}_B , calculated from \mathbf{X}' .

In the same way that for Gaussian classifier, as the vectors produced by the DFA of vibration signals are selected to define the sets of training and testing, and a discussion about the success rate of Karhunen-Love transformation in identification of each unbalancing level studied is made below in Section 5.4.

5.4. Signal classification

This section shows the results concerning the training and testing steps performed with the three classifiers. First, we regarded the three main classes of signals: (1) unbalancing by mass addition at one blade; (2) lack of mass at one blade; and (3) balanced system. Table 2 present the results from different classifiers using these three classes. For all of these cases and for each used classifier, 80% (320) of the 400 available vectors processed by

the DFA were selected randomly to define the training set, using the 20% (80) remaining vectors to define the testing stage. The purpose of the test data is to evaluate the performance of the classifier for data that were not used during the training, i.e. its generalizability. Averages were taken over 100 distinct choices of training and testing sets.

During the signals collection two subsets of signals associated to the balanced system condition were recorded. One of them was acquired with three balanced blades and another one without the blades (shaft only). The purpose was to test the balance of the shaft as well as that of the whole system. If every part of system (shaft and blades) is balanced, one can conclude that the vibration levels of both subsets are similar, and the corresponding signals will have the same classification.

Table 2 shows clearly that the overall average for the training process (100%, 98.37% and 99.96%) is higher than for the test process (99.79%, 97.68% and 99.83%). This is so because it is easier to classify a data that was supplied to the classifier during the training process.

It should be stressed that all vectors associated to a balanced system were perfectly classified, demonstrating that the three pattern recognition techniques' output is that the balanced blades and only shaft both represent a single class. Both neural network and KLT yielded good results as an overall average precision of over 99% was achieved. The performance of the Gaussian classifier was only slightly inferior to the other ones, but with the advantage of an easier implementation. Around 5% of the signals belonging to class two were misclassified as belonging to class one during testing stage. The same misclassification occurred during training, but with an average percentage error of 4.35%. Table 2 shows the classification success rate obtained by neural network, Gaussian classifier and Karhunen-Loève transformation when classifying those groups.

It notorious that when the training procedure of the classifiers is done with only three major work conditions, it is not possible to distinguish all the different sublevels of wind turbine imbalance. Therefore, the training and test processes of classifiers were repeated for seven independent classes. The seven classes are formed by the following subsets: classes 1 to 3 representing 0.5, 1.0 and 1.5 g added at one blade; classes 4 to 6 representing 0.5, 1.0 and 1.5 g added at two blades; and class 7 representing three balanced blades plus shaft only. The success rate achieved for the three classifiers using seven subsets of signals are presented on Table 3.

From results shown on Table 3, it is possible to determine the degree of confusion between different imbalance levels.

Once more, the overall average for training process (99.96%, 100% and 100%) is higher than for test process (98.67%, 99.31% and 99.88%). Also, the subsets of signals acquired under balanced condition were correctly classified as a single class. By these results, despite of a blockage ratio of 50.77% and a blockage factor of 0.84, it is observed that there was no change in vibration measurement standard and that the classifiers could not distinguish the condition of three balanced blades from the shaft-only case. A similar conclusion can be drawn regarding the surface roughness of the blade and a possible stall of the wind tunnel fan.

By analyzing the errors occurred during the classification shown in Table 3, it can be seen that the worst misclassification occurred when 3.9% of vectors belonging to class 4 (two blades with 0.5 g) were misclassified as belonging to class 5 (two blades with 1.0 g). Likewise, 3.5% of vectors belonging to class 5 were misclassified as belonging to class 4. Furthermore, another high misclassification (2.6%) occurred when vectors from class 3 (one blade with 1.5 g) were mistakenly classified as from class 6 (two blades with 1.5 g) and vice-versa (0.6%). It must be pointed out that 1.5 g added represents 10% of an individual blade weight, therefore a severely unbalanced state is produced. This, then, is a possible reason for these mistakes.

In general, KLT showed higher average success rate, followed by the Gaussian classifier. Despite of this, all classifiers presented good results, being able to identify imbalance levels with high accuracy.

6. Conclusion

The automatic classification using k-means, an unsupervised learning algorithm, suggests the existence of four classes. This optimum number of classes gives us another idea about how to group different imbalance levels, which is possibly related to the amount of mass added to the system. Whatever the case may be, we concluded it is possible to classify different imbalance levels. With the combination of Detrended Fluctuation Analysis and pattern recognition techniques, it is possible to predict the best moment to carry out maintenance services, reducing costs and maintenance time.

K-means, which is an unsupervised technique, held a classification where classes with similar levels of vibration have been joined together to form 4 groups. However, as some groups are composed by more than one class, this classification does not allow an accurate diagnosis about the present defects.

The classifiers implemented by neural networks, Gaussian classifier and Karhunen-Loève transform were very efficient to classify vibration signals according to different imbalance levels in a scaled wind turbine.

The best accuracy rates for three imbalance levels were obtained using the Neural network (with 100% and 99.79% of success for training and testing, respectively), followed by the Karhunen-Loève classifier (with 99.96% and 99.83%) and the Gaussian classifier (with 98.37% and 97.68%). For seven unbalancing levels, the best results were obtained using the Karhunen-Loève classifier (with 100% and 99.88% of success for training and testing, respectively), followed by the Gaussian classifier (with 100% and 99.31%) and the Neural network (with 99.96% and 98.67%). Above all, the balanced condition was well classified for all methods applied, both unsupervised and supervised, with 100% precision. It is important to point out that the performances of all classifiers are similar and the standard deviations calculated over one hundred sets of training and testing vectors were never superior to 5% in any of the experiments. These results show the capability of classifiers to identify the imbalance levels of new data.

Based on the presented results, we can conclude that the Karhunen-Loève classifier has the highest accuracy, being able to accurately distinguish all induced imbalances. Thus, this method showed to be the most appropriate tool for use in the maintenance of wind turbine blades. Despite that KL classifier has been the most accurate, neural networks and Gaussian classifiers also achieved excellent results, with averages of hits greater than 97%. With such precision, these results give important contributions to the development of an automatic system for unbalance diagnosis in wind turbines.

Acknowledgements

We gratefully acknowledge the financial support of the Brazilian agencies CAPES, FUNCAP and CNPq.

References

- [1] A. Abouhnik, A. Albarbar, Wind turbine blades condition assessment based on vibration measurements and the level of an empirically decomposed feature, *Energy Convers. Manag.* 64 (2012) 606–613 (IREC) 2011, The International Renewable Energy Congress.
- [2] L. Barelli, G. Bidini, F. Bonucci, E. Moretti, The radiation factor computation of energy systems by means of vibration and noise measurements: the case study of a cogenerative internal combustion engine, *Appl. Energy* 100 (2012) 258–266 (clean Energy for Future Generations).
- [3] T. Burton, D. Sharpe, N. Jenkins, E. Bossanyi, *Wind Energy Handbook*, John Wiley & Sons, 2001.
- [4] A. Carbone, G. Castelli, H. Stanley, Time-dependent hurst exponent in financial time series, *Phys. A Stat. Mech. Appl.* 344 (12) (2004) 267–271 applications of Physics in Financial Analysis 4 (APFA4), <http://www.sciencedirect.com/science/article/pii/S0378437104009471>.
- [5] T. Chen, L. Liou, Blockage corrections in wind tunnel tests of small horizontal-axis wind turbines, *Exp. Therm. Fluid Sci.* 35 (3) (2011) 565–569. <http://www.sciencedirect.com/science/article/pii/S0894177710002438>.
- [6] G. Cybenko, Approximation by superpositions of a sigmoidal function. *Mathematics of Control, Signals Syst.* 2 (4) (1989) 303–314.
- [7] D. Daniher, L. Briens, A. Tallevi, End-point detection in high-shear granulation using sound and vibration signal analysis, *Powder Technol.* 181 (2) (2008) 130–136 (particulate Processes in the Pharmaceutical Industry).
- [8] David L. Davies and Donald W. Bouldin, A cluster separation measure, *IEEE Trans. Pattern Anal. Mach. Intell.* PAMI-1 (2), 224–227, ISSN: 0162-8828, DOI: 10.1109/TPAMI.1979.4766909.
- [9] M.S. de Almeida, Implementação computacional para desenvolvimento de pás de turbinas eólicas de eixo horizontal (in portuguese), Master's thesis, Universidade Federal do Ceará, 2013.
- [10] E. de Moura, P. Normando, L. Gonçalves, S. Kruger, Characterization of cast iron microstructure through fluctuation and fractal analyses of ultrasonic backscattered signals combined with classification techniques, *J. Nondestruct. Eval.* 31 (1) (2012) 90–98.
- [11] E. de Moura, C. Souto, A. Silva, M. Irmão, Evaluation of principal component analysis and neural network performance for bearing fault diagnosis from vibration signal processed by {RS} and {DF} analyses, *Mech. Syst. Signal Process.* 25 (5) (2011) 1765–1772.
- [12] E. de Moura, A. Vieira, M. Irmão, A. Silva, Applications of detrended-fluctuation analysis to gearbox fault diagnosis, *Mech. Syst. Signal Process.* 23 (3) (2009) 682–689.
- [13] N.D. Duc, T.Q. Quan, V.D. Luat, Nonlinear dynamic analysis and vibration of shear deformable piezoelectric {FGM} double curved shallow shells under damping-thermo-electro-mechanical loads, *Compos. Struct.* 125 (2015) 29–40.
- [14] Z. Feng, M.J. Zuo, Fault diagnosis of planetary gearboxes via torsional vibration signal analysis, *Mech. Syst. Signal Process.* 36 (2) (2013) 401–421.
- [15] J. Finn, J. Wagner, H. Bassily, Monitoring strategies for a combined cycle electric power generator, *Appl. Energy* 87 (8) (2010) 2621–2627.
- [16] B. Fitzgerald, B. Basu, Cable connected active tuned mass dampers for control of in-plane vibrations of wind turbine blades, *J. Sound Vib.* 333 (23) (2014) 5980–6004.
- [17] F. Gonzalez-Longatt, P. Wall, V. Terzija, Wake effect in wind farm performance: steady-state and dynamic behavior, *Renew. Energy* 39 (1) (2012) 329–338.
- [18] S. Haykin, *Neural Networks: a Comprehensive Foundation* (International edition. Prentice Hall), 1999.
- [19] R. Hecht-Nielsen, Kolmogorovs mapping neural network existence theorem, in: *Proceedings of the International Conference on Neural Networks*, 3, IEEE Press, New York, 1987, pp. 11–14.
- [20] K. Hornik, M. Stinchcombe, H. White, Multilayer feedforward networks are universal approximators, *Neural Netw.* 2 (5) (1989) 359–366.
- [21] H.D. Jennings, P.C. Ivanov, A. de M. Martins, P. da Silva, G. Viswanathan, Variance fluctuations in nonstationary time series: a comparative study of

- music genres, *Phys. A Stat. Mech. its Appl.* 336 (34) (2004) 585–594. <http://www.sciencedirect.com/science/article/pii/S037843710301241X>.
- [22] M.L. Kurnaz, Detrended fluctuation analysis as a statistical tool to monitor the climate, *Journal of Statistical Mechanics: Theory and Experiment* 2004 (07) (2004) P07009. <http://stacks.iop.org/1742-5468/2004/i=07/a=P07009>.
- [23] M. Liu, H. Xia, L. Sun, B. Li, Y. Yang, Vibration signal analysis of main coolant pump flywheel based on hilberthuang transform, *Nucl. Eng. Technol.* 47 (2) (2015) 219–225 special Issue on ISOFIC/ISSNP2014.
- [24] W. Liu, The vibration analysis of wind turbine bladecabintower coupling system, *Eng. Struct.* 56 (2013) 954–957.
- [25] S. Lloyd, Least squares quantization in pcm, *Information Theory, IEEE Trans.* 28 (2) (Mar 1982) 129–137.
- [26] J.O. Matos, E.P. de Moura, S.E. Krger, J.A. Rebello, Rescaled range analysis and detrended fluctuation analysis study of cast irons ultrasonic backscattered signals, *Chaos, Solit. Fractals* 19 (1) (2004) 55–60. <http://www.sciencedirect.com/science/article/pii/S0960077903000808>.
- [27] O.D. Mohammed, M. Rantatalo, J.-O. Aidanp, U. Kumar, Vibration signal analysis for gear fault diagnosis with various crack progression scenarios, *Mech. Syst. Signal Process.* 41 (12) (2013) 176–195.
- [28] P.G. Normando, R. a. S. Nascimento, E.P. Moura, A.P. Vieira, Microstructure identification via detrended fluctuation analysis of ultrasound signals, *Phys. Rev. E* 87 (Apr 2013) 043304.
- [29] L.R. Padovese, F.E. da Silva, E.P. Moura, L.L. Goncalves, Characterization of microstructural changes in coarse ferriticpearlitic stainless steel through the statistical fluctuation and fractal analyses of barkhausen noise, *AIP Conf. Proc.* 1211 (1) (2010) 1293–1300, in: <http://scitation.aip.org/content/aip/proceeding/aipcp/10.1063/1.3362217>.
- [30] K. Pearson, On lines and planes of closest fit to systems of points in space, *Philos. Mag. Ser. 6* 2 (11) (1901) 559–572.
- [31] C.-K. Peng, S.V. Buldyrev, S. Havlin, M. Simons, H.E. Stanley, A.L. Goldberger, Mosaic organization of dna nucleotides, *Phys. Rev. E* 49 (Feb 1994 a) 1685–1689.
- [32] C.-K. Peng, S.V. Buldyrev, S. Havlin, M. Simons, H.E. Stanley, A.L. Goldberger, Mosaic organization of dna nucleotides, *Phys. Rev. E* 49 (Feb 1994 b) 1685–1689. <http://link.aps.org/doi/10.1103/PhysRevE.49.1685>.
- [33] Z. Peng, P.W. Tse, F. Chu, An improved hilberthuang transform and its application in vibration signal analysis, *J. Sound Vib.* 286 (12) (2005) 187–205.
- [34] Z. Peng, W. Zhang, Z. Lang, G. Meng, F. Chu, Timefrequency data fusion technique with application to vibration signal analysis, *Mech. Syst. Signal Process.* 29 (2012) 164–173.
- [35] B. Podobnik, H.E. Stanley, Detrended cross-correlation analysis: a new method for analyzing two nonstationary time series, *Phys. Rev. Lett.* 100 (Feb 2008) 084102.
- [36] A. Puchalski, A technique for the vibration signal analysis in vehicle diagnostics, *Mech. Syst. Signal Process.* 5657 (2015) 173–180.
- [37] L. Rokach, O. Maimon, Clustering methods, in: O. Maimon, L. Rokach (Eds.), *Data Mining and Knowledge Discovery Handbook*, Springer, US, 2005, pp. 321–352.
- [38] P.J. Rousseeuw, Silhouettes: a graphical aid to the interpretation and validation of cluster analysis, *J. Comput. Appl. Math.* 20 (1987) 53–65.
- [39] A. Singh, A. Yadav, A. Rana, K-means with three different distance metrics, *Int. J. Comput. Appl.* 67 (10) (April 2013) 13–17.
- [40] A. Staino, B. Basu, Dynamics and control of vibrations in wind turbines with variable rotor speed, *Eng. Struct.* 56 (2013) 58–67.
- [41] L. Telesca, V. Lapenna, M. Macchiato, Mono- and multi-fractal investigation of scaling properties in temporal patterns of seismic sequences, *Chaos, Solit. Fractals* 19 (1) (2004) 1–15. <http://www.sciencedirect.com/science/article/pii/S0960077903001887>.
- [42] A. Vieira, E. de Moura, L. Goncalves, J. Rebello, Characterization of welding defects by fractal analysis of ultrasonic signals, *Chaos Solit. Fractals* 38 (3) (2008) 748–754. <http://www.sciencedirect.com/science/article/pii/S0960077907000306>.
- [43] A.P. Vieira, H.H.M. Vasconcelos, L.L. Goncalves, H.C. de Miranda, Fractal analysis of metal transfer in mig/mag welding, *AIP Conf. Proc.* 1096 (1) (2009) 564–571, in: <http://scitation.aip.org/content/aip/proceeding/aipcp/10.1063/1.3114305>.
- [44] P. Wasserman, *Neural Computing: Theory and Practice*. A Van Nostrand Reinhold Book, Van Nostrand Reinhold, 1989.
- [45] A. Webb, *Statistical Pattern Recognition*, Wiley, 2002.
- [46] J. Xun, S. Yan, A revised hilberthuang transformation based on the neural networks and its application in vibration signal analysis of a deployable structure, *Mech. Syst. Signal Process.* 22 (7) (2008) 1705–1723.
- [47] Z. Zhang, J. Li, S.R. Nielsen, B. Basu, Mitigation of edgewise vibrations in wind turbine blades by means of roller dampers, *J. Sound Vib.* 333 (21) (2014) 5283–5298.
- [48] M. Zhao, J. Ji, Nonlinear torsional vibrations of a wind turbine gearbox, *Appl. Math. Model.* 39 (16) (2015) 4928–4950.